iJRASET
International Journal For Research in
Applied Science and Engineering Technology

INTERNATIONAL JOURNAL FOR RESEARCH
IN APPLIED SCIENCE & ENGINEERING TECHNOLOGY

Volume: 13 Issue: XII Month of publication: December 2025

DOI: https://doi.org/10.22214/ijraset.2025.76649

International Journal for Research in Applied Science & Engineering Technology (IJRASET)
ISSN: 2321-9653; IC Value: 45.98; SJ Impact Factor: 7.538
Volume 13 Issue XII Dec 2025- Available at www.ijraset.com

Analysis of Cosmic Ray Intensity Variations with Solar and Solar Wind Parameters in Solar Cycles 23 and 24

Jitendra Satnami[1], Achyut Pandey[2], Deepak K Chaurasiya[3], C.M. Tiwari[4]
[1]*Research Scholar Department of Physics, APS University, Rewa*
[2]*Professor Department of Physics, TRS College Rewa*
[3]*Guest Faculty Department of Physics, BBM Govt College Divyagawan, Rewa*
[4]*Assistant Professor Department of Physics, APS University, Rewa*

Abstract: The intensity of GCRs is strongly modulated by solar and interplanetary conditions and varies systematically with the solar activity cycle. In this study, cosmic ray intensity variations during Solar Cycles 23 and 24 are investigated using neutron monitor data from Oulu and Moscow stations, representing different cutoff rigidities. The observations are analysed in conjunction with solar and Solar wind parameters, including Rz, SRF, V_{SP}, T_{SP} and D_{SP} . GCR intensity and solar activity are found to be strongly anti-correlated, with much greater modulation during Solar Cycle 23 than during the weaker Solar Cycle 24. There are clear stiffness-dependent effects, with increased modulation at lower cutoff rigidity. Transient solar disturbances are also linked to short-term reductions. These findings advance knowledge of cosmic ray modification in the heliosphere that is dependent on the solar cycle.
Keywords: Cosmic rays, Solar cycle, Solar Wind Parameters, Galactic cosmic ray modulation, Neutron Monitor.

I. INTRODUCTION

Galactic cosmic rays (GCRs), are highly energetic charged particles originating outside the solar system, undergo significant modulation as they propagate through the heliosphere. The intensity of GCRs observed near Earth exhibits a well-established anti-phase relationship with the 11-year solar activity cycle (Forbush, 1954; Hatton, 1980). Variations in solar activity modify the solar wind and interplanetary magnetic field (IMF), thereby influencing cosmic ray transport through processes such as diffusion, convection, gradient and curvature drifts, and adiabatic deceleration (Parker, 1965; Kota, 2013; Zhao, 2014).

Solar activity is commonly quantified using indices such as sunspot number (Rz) and 10.7 cm solar radio flux (SRF), which are reliable proxies for changes in the solar magnetic field. In addition to long-term modulation, transient solar phenomena including solar flares, coronal mass ejections (CMEs), and high-speed solar wind streams originating from coronal holes produce short-term disturbances in the interplanetary medium. These disturbances often result in sudden decreases in cosmic ray intensity, known as Forbush decreases (Shea and Smart, 1985; Mavromichalaki et al., 2007; Shrivastava et al., 1996, 2001).

The lagged response of cosmic ray intensity relative to solar activity indices was first reported by Forbush (1958) and subsequently confirmed by Simpson (1963), indicating the cumulative nature of heliospheric modulation processes. More recent studies suggested long-term modulation trends may be better explain by incorporating heliospheric magnetic field parameters, particularly variations in the solar polar magnetic fields (Shrivastava, 2011).

Solar Cycles 23 & 24 represent distinctly different phases of solar activity, with Solar Cycle 24 being significantly weaker than Solar Cycle 23. This contrast given a valuable opportunity to examine how varying solar and interplanetary conditions influence cosmic ray modulation. In the present study, long-term variations in cosmic ray intensity are analyzed using neutron monitor data from Oulu and Moscow stations, representing different cutoff rigidities. The cosmic ray observations are examined in relation to multiple solar and interplanetary parameters during Solar Cycles 23 and 24 to better understand the dependence of cosmic ray modulation on solar cycle strength and heliospheric conditions.

II. DATA AND METHODOLOGY

A. Dataset

The present study utilizes long-term cosmic ray intensity (CRI) data obtained from ground-based neutron monitor (NM) stations to investigate modulation effects during Solar Cycles 23 and 24. Neutron monitor data from Oulu (cutoff rigidity ≈ 0.8 GV) and Moscow (cutoff rigidity ≈ 2.4 GV) stations are used, representing low and mid cutoff rigidity regions, respectively. These stations are selected to examine rigidity-dependent modulation effects in cosmic ray intensity.

To characterize solar activity, several widely used parameters were employed, including sunspot number (Rz), 10.7 cm solar radio flux (SRF), and coronal mass ejection (CME) occurrence rates. In addition, key solar wind parameters were considered, namely solar plasma speed (VSP), solar proton temperature (TSP), and solar plasma density (DSP). These parameters collectively represent the large-scale heliospheric conditions that influence cosmic ray transport.

B. Methodology

Monthly and annual mean values of cosmic ray intensity and solar/interplanetary parameters were analyzed to minimize short-term fluctuations and emphasize long-term modulation trends. The statistical relationship between CRI and each solar or interplanetary parameter was quantified using Pearson's correlation coefficient (r). Furthermore, linear regression analysis was performed to examine the dependence of solar and interplanetary parameters on cosmic ray intensity, expressed as

$$Y = \alpha + \beta.CRI$$

where Y denote the solar or interplanetary parameter, α is intercept & β is regression coefficient. Hypothesis testing was carried out at the 5% significance level to assess the statistical significance of the correlation and regression coefficients.

III. OBSERVATIONAL RESULTS & ANALYSIS

A. Long Term Association of CRI & RZ

Long-term cosmic ray variation is still an intriguing area of study in space science. Many researchers (Lange & Forbush, 1957; Shea and Smart, 1985; Shrivastava et al,1993; Mavaromichalaki et al, 2007) have invested the last six to seven decades researching the solar modulation of cosmic rays. In order to determine the long-term relationship between cosmic rays and solar activity, we used sunspot numbers in our investigation. In 1954, Forbush discovered a negative link between the number of sunspots and cosmic rays.

Figures 1.1 and 1.2 present the temporal variations of monthly and annual mean cosmic ray intensity recorded at the Oulu and Moscow neutron monitor stations in relation to sunspot numbers during Solar Cycles 23 and 24 (1996–2019). A clear antiphase relationship between sunspot activity and cosmic ray intensity is observed, consistent with solar cycle modulation. While the minimum cosmic ray intensity closely corresponds to the maximum sunspot activity during Solar Cycle 23, such a one-to-one correspondence is not evident for annual mean values during Solar Cycle 24. The presence of two distinct minima in cosmic ray intensity during Solar Cycle 23 further reflects the complex modulation processes operating during periods of enhanced solar activity. The analysis also indicates that Solar Cycle 23 exhibits a larger amplitude compared to the weaker Solar Cycle 24.

Figures 1.3 and 1.4 show the correlation between annual mean sunspot number (SSN, Rz) and cosmic ray intensity for both neutrons monitor stations. A strong negative correlation is found during both solar cycles, with correlation coefficients of −0.86 (Oulu) and −0.85 (Moscow) for Solar Cycle 23, and −0.94 and −0.95 for Solar Cycle 24. The differing regression slopes between the two cycles suggest variations in modulation efficiency, highlighting the influence of changing heliospheric conditions across successive solar cycles.

The linear model is represented by the equation for linear regression:

$$R_Z = \alpha + \beta.CRI$$

Figures 1.3 and 1.4 show that the regression (trend) line for Solar Cycle 24 is lower than that for Solar Cycle 23, indicating weaker modulation during the later cycle. The coefficient of determination reveals that sunspot number explains approximately 74% and 72% of the variability in cosmic ray intensity recorded at the Oulu and Moscow stations, respectively, during Solar Cycle 23, and about 88% and 90% during Solar Cycle 24. These values indicate a good fit between the model and the observed data. Hypothesis testing performed at the 5% significance level confirms that the regression coefficients are statistically significant at the 95% confidence level.

B. Long Term Association of CRI & SRF –

The long-term variation of the F10.7 cm solar radio flux (SRF) shows a strong association with changes in cosmic ray intensity. The F10.7 index is widely regarded as a reliable indicator of global solar activity, representing disk-integrated solar emission at a radio wavelength of 10.7 cm (2800 MHz). It exhibits variability similar to that of sunspot numbers and serves as an effective proxy for solar magnetic activity. As shown in Figures 1.5 and 1.6, the radio flux reaches higher values during Solar Cycle 23 compared to the weaker Solar Cycle 24.

International Journal for Research in Applied Science & Engineering Technology (IJRASET)
ISSN: 2321-9653; IC Value: 45.98; SJ Impact Factor: 7.538
Volume 13 Issue XII Dec 2025- Available at www.ijraset.com

Figures 1.7 and 1.8 present the correlation between annual mean F10.7 solar radio flux and cosmic ray intensity measured by the Oulu and Moscow neutron monitor stations during Solar Cycles 23 and 24. A strong inverse relationship is observed in both cycles, with correlation coefficients of −0.86 (Oulu) and −0.84 (Moscow) during Solar Cycle 23, and −0.95 and −0.96 during

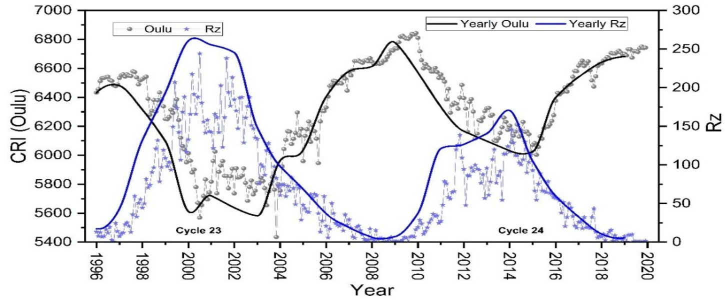

Fig 1. 1 Time profile of monthly average and yearly average values of SSN (R_Z) with cosmic ray intensity variation (Oulu Neutron monitor) during solar cycle 23 and 24

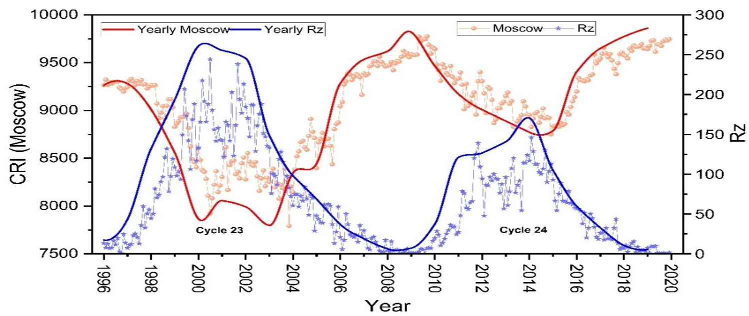

Fig 1. 2 Time profile of monthly average and yearly average values of SSN (R_Z) with cosmic ray intensity variation (Moscow Neutron monitor) during solar cycle 23 and 24

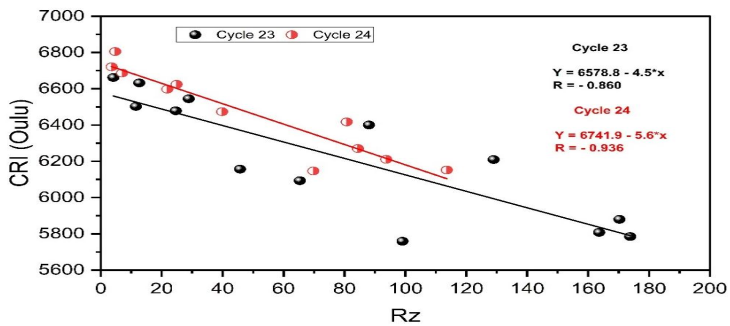

Fig 1. 3 Correlation profile of the yearly average value of SSN (R_Z) with cosmic ray intensity variation (Oulu Neutron monitor) during solar cycle 23 and 24

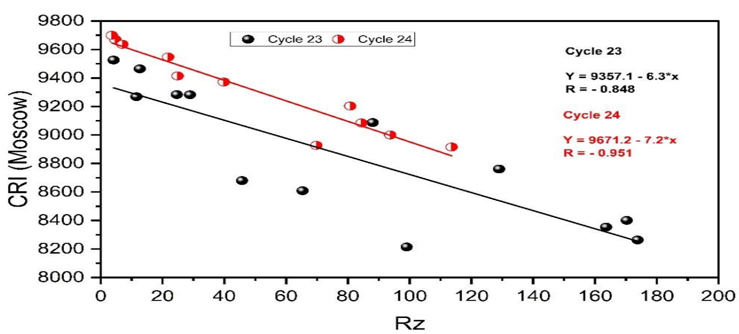

Fig 1. 4 Correlation profile of the yearly average value of SSN (R_Z) with cosmic ray intensity variation (Moscow) during solar cycle 23 and 24

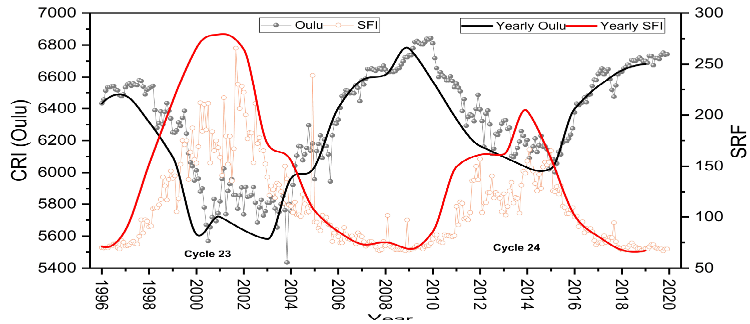

Fig 1. 5 Time profile of monthly average and yearly average values of F10.7 solar radio flux (SRF) with cosmic ray intensity variation (Oulu Neutron monitor) during solar cycle 23 and 24

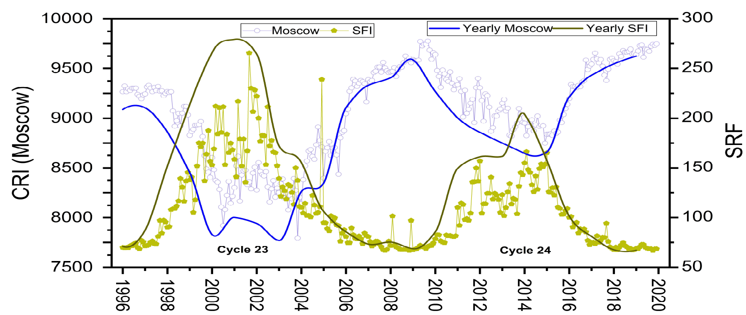

Fig 1. 6 Time profile of monthly average and yearly average values of F10.7 solar radio flux (SRF) with cosmic ray intensity variation (Moscow Neutron monitor) during solar cycle 23 and 24

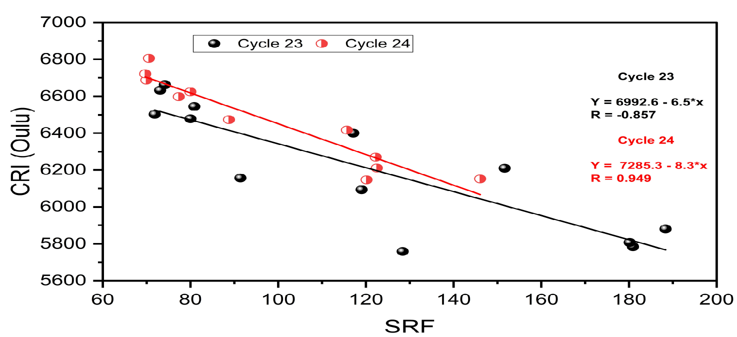

Fig 1. 7 Correlation profile of the yearly average value of F10.7 solar radio flux (SRF) with cosmic ray intensity variation (Oulu Neutron monitor) during solar cycle 23 and 24

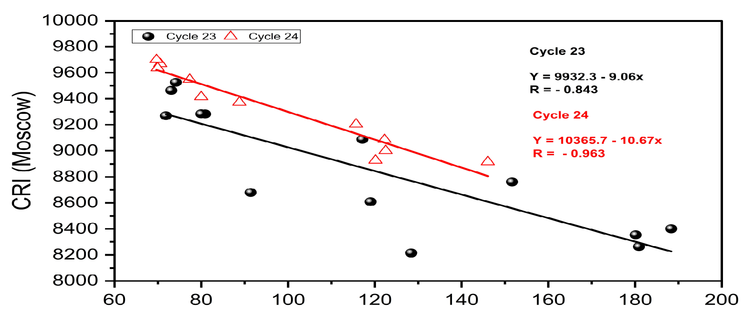

Fig 1. 8 Correlation profile of the yearly average value of F10.7 solar radio flux (SRF) with cosmic ray intensity variation (Moscow Neutron monitor) during solar cycle 23 and 24

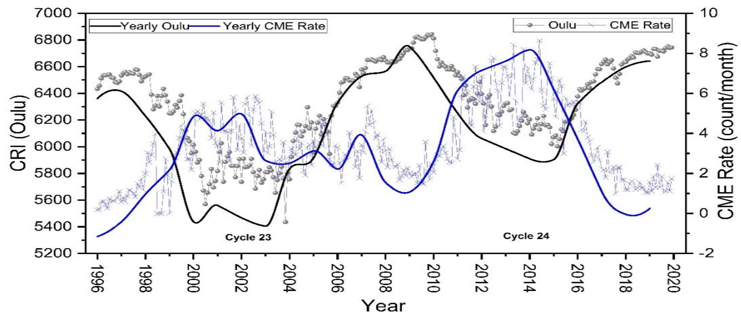

Fig 1. 9 Time profile of monthly average and yearly average values of CME rate with cosmic ray intensity variation (Oulu Neutron monitor) during solar cycle 23 and 24

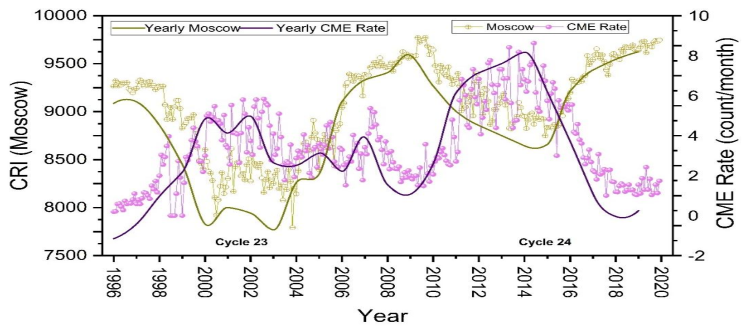

Fig 1. 10 Time profile of monthly average and yearly average values of CME rate with cosmic ray intensity variation (Moscow Neutron monitor) during solar cycle 23 and 24

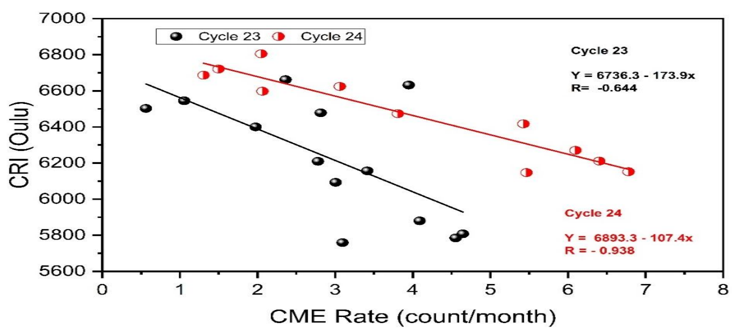

Fig 1. 11 Correlation profile of the yearly average value of CME rate with cosmic ray intensity variation (Oulu Neutron monitor) during solar cycle 23 & 24

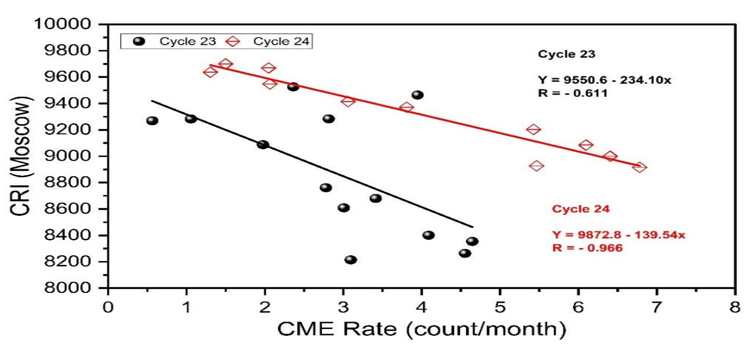

Fig 1. 12 Correlation profile of the yearly average value of CME rate with cosmic ray intensity variation (Moscow Neutron monitor) during solar cycle 23 & 24

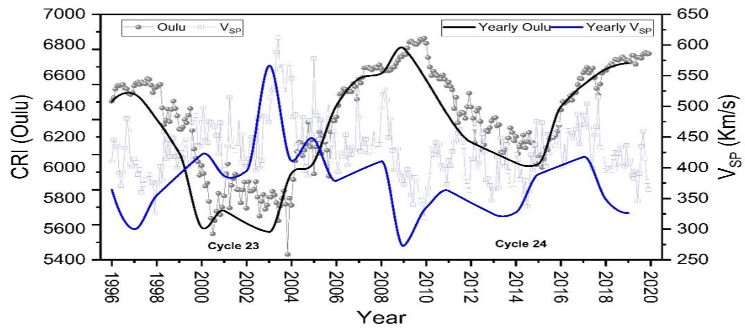

Fig 1. 13 Time profile of monthly average and yearly average values of Solar plasma velocity (V_{SP}) with cosmic ray intensity variation (Moscow Neutron monitor) during solar cycle 23 and 24

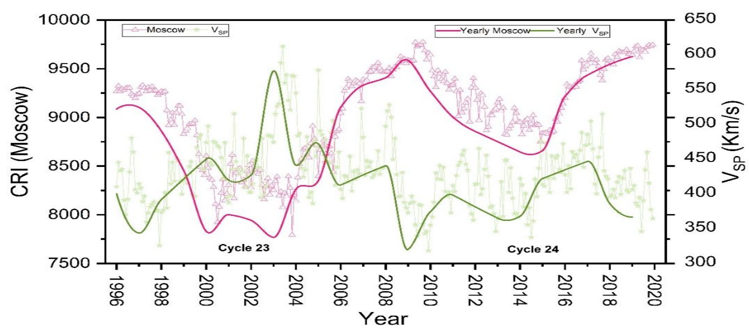

Fig 1. 14 Time profile of monthly average and yearly average values of Solar plasma velocity (V_{SP}) with cosmic ray intensity variation (Moscow Neutron monitor) during solar cycle 23 and 24

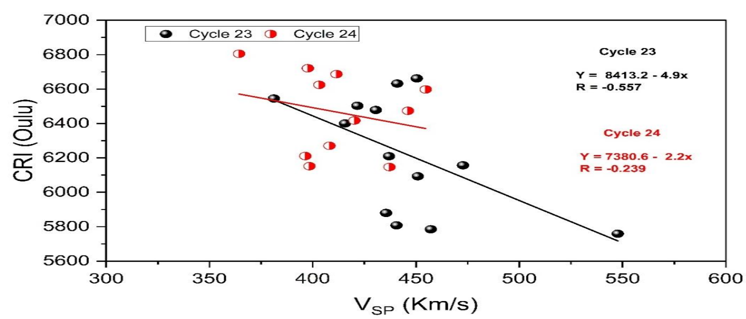

Fig 1. 15 Correlation profile of the yearly average value of Solar plasma speed (V_{SP}) with cosmic ray intensity variation (Oulu Neutron monitor) during solar cycle 23 and 24

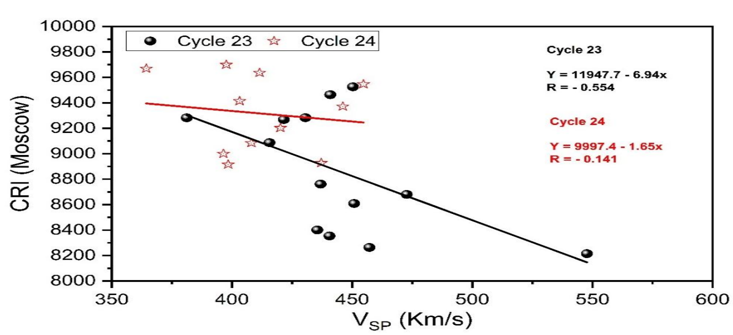

Fig 1. 16 Correlation profile of the yearly average value of Solar plasma speed (V_{SP}) with cosmic ray intensity variation (Moscow Neutron monitor) during solar cycle 23 and 24

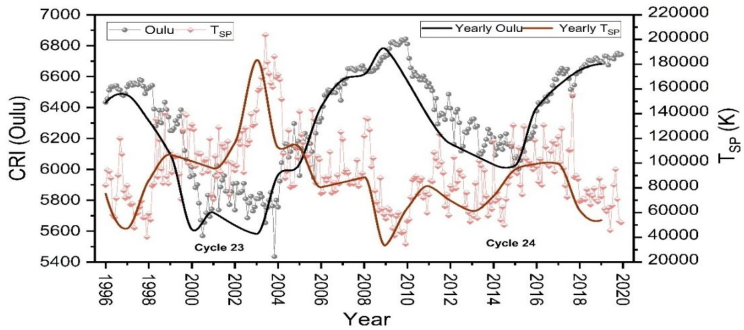

Fig 1. 17 Time profile of monthly average and yearly average values of Solar plasma temperature (T_{SP}) with cosmic ray intensity variation (Oulu Neutron monitor) during solar cycle 23& 24

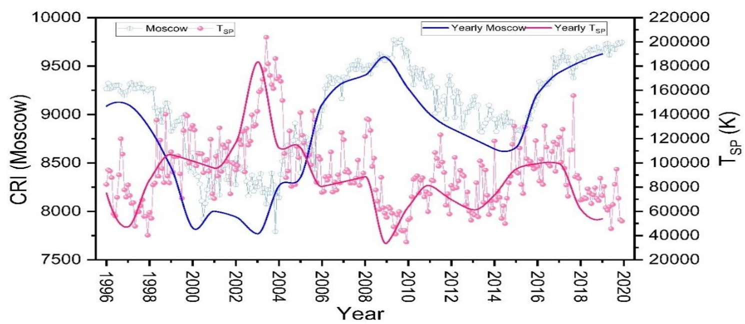

Fig 1. 18 Time profile of monthly average and yearly average values of Solar plasma temperature (T_{SP}) with cosmic ray intensity variation (Moscow Neutron monitor) during solar cycle 23&24

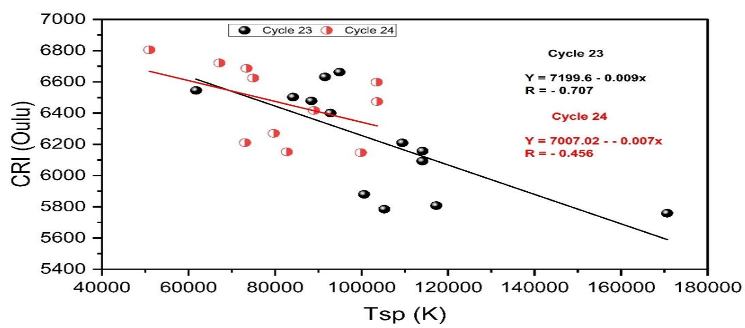

Fig 1. 19 Correlation profile of the yearly average value of Solar proton temperature (T_{SP}) with cosmic ray intensity variation (Oulu Neutron monitor) during solar cycle 23 and 24

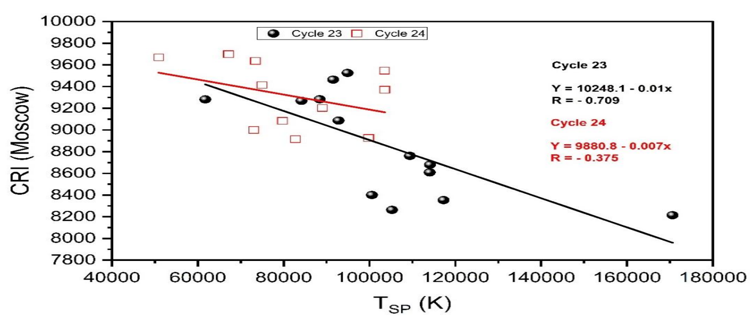

Fig 1. 20 Correlation profile of the yearly average value of Solar proton temperature (T_{SP}) with cosmic ray intensity variation Moscow Neutron monitor) during solar cycle 23 and 24

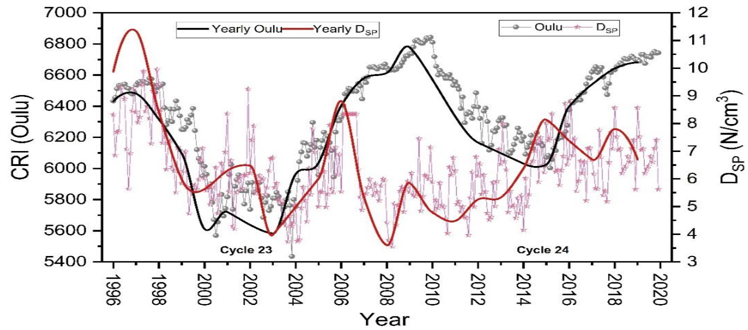

Fig 1. 21 Time profile of monthly average and yearly average values of Solar plasma density (D_{SP}) with cosmic ray intensity variation (Oulu Neutron monitor) during solar cycle 23 and 24

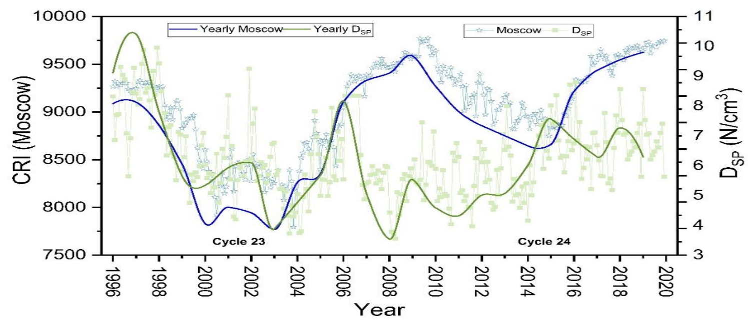

Fig 1. 22 Time profile of monthly average and yearly average values of Solar plasma density (D_{SP}) with cosmic ray intensity variation (Moscow Neutron monitor) during solar cycle 23 and 24

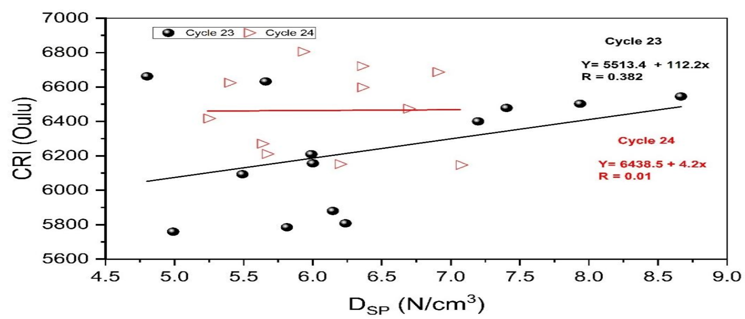

Fig 1. 23 Correlation profile of the yearly average value of Solar proton density (D_{SP}) with cosmic ray intensity variation (Oulu Neutron monitor) during solar cycle 23 and 24

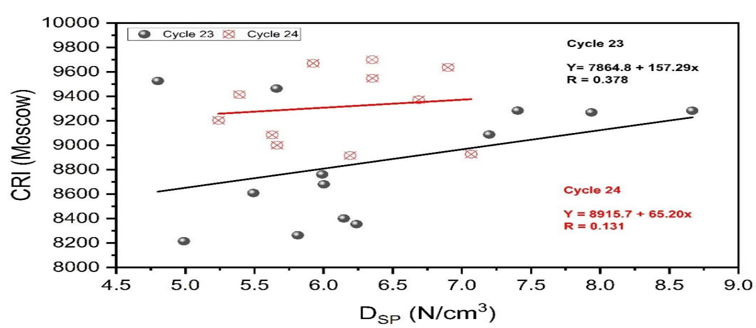

Fig 1. 24 Correlation profile of the yearly average value of Solar proton density (D_{SP}) with cosmic ray intensity variation (Moscow Neutron monitor) during solar cycle 23 and 24

Solar Cycle 24, respectively. The coefficient of determination indicates that SRF accounts for approximately 74% and 71% of the cosmic ray intensity variability during Solar Cycle 23, and about 90% and 93% during Solar Cycle 24 for the Oulu and Moscow stations, respectively, demonstrating a good model fit. Hypothesis testing performed at the 5% significance level confirms that all regression coefficients are statistically significant at the 95% confidence level.

Consistent with earlier studies (Singh et al., 2016; Bhattacharya and Roy, 2014), these results confirm that the F10.7 solar radio flux is a robust and effective solar activity parameter for analysing long-term variations in cosmic ray intensity.

C. Long Term Association of CRI & CME Rates

Coronal mass ejections (CMEs) are large-scale magnetized plasma structures that originate from the Sun's closed magnetic field regions and propagate into interplanetary space, particularly throughout the heliosphere. The daily occurrence rate of CMEs (typically less than 0.5 events per day) has been examined using extensive observational data. CME occurrence rates show significant variability over short timescales and exhibit modulation patterns similar to those of the solar cycle.

Recent studies have demonstrated the influence of CMEs on variations in cosmic ray intensity (Cane, 2000; Lara et al., 2005). Shrivastava (2007) and Mishra et al. (2005) further reported both short-term and long-term effects of CMEs on the modulation of galactic cosmic rays. In the present study, the annual mean cosmic ray intensities recorded at the Oulu and Moscow neutron monitor stations were analysed in relation to CME occurrence rates.

Figures 1.9 and 1.10 present time-series profiles of the monthly and annual mean CME rates alongside the corresponding variations in cosmic ray intensity measured by the Oulu and Moscow neutron monitors during solar cycles 23 and 24. Annual CME rates were derived by considering all recorded CME events. The figures clearly reveal an approximately 11-year cyclic variation consistent with the solar cycle. Solar cycle 23 exhibits multiple peaks in CME activity, whereas solar cycle 24 shows a comparatively higher amplitude in CME rates.

Figures 1.11 and 1.12 depict the correlation between variations in cosmic ray intensity (from the Oulu and Moscow neutron monitors) and the annual mean CME rates during solar cycles 23 and 24. A strong negative correlation is observed, with correlation coefficients of −0.64 and −0.61 for the Oulu and Moscow stations, respectively, during solar cycle 23, and −0.94 and −0.97 during solar cycle 24. These results indicate a significantly stronger inverse relationship between CME activity and cosmic ray intensity during solar cycle 24. The corresponding linear regression equations are given by:

$$\text{CME rate} = \alpha+\beta*\text{CRI},$$

where α is the intercept and β is the slope.

For solar cycles 23 and 24, the CME rate accounts for approximately 41%, 37%, 88%, and 93% of the variability in the CRI data from Oulu and Moscow, respectively. These results demonstrate the strong predictive capability of the model. Hypothesis testing was conducted at the 5% level of significance, and both coefficients were found to be statistically significant at the 95% confidence level.

D. Long Term Association of CRI & V_{SP}

Numerous studies have examined the long-term variation of cosmic ray intensity (CRI) and its relationship with solar wind parameters. Forbush (1985) was among the first to identify an inverse correlation between solar wind stream velocity and long-term cosmic ray variations. According to diffusion–convection theory, CRI varies with solar wind speed. The primary mechanisms responsible for cosmic ray modulation include convection by the radially expanding solar wind, diffusion within the heliospheric magnetic field, particle drift caused by magnetic field irregularities, and changes in particle momentum (Parker, 1965; Sabbah, 2000; Bazilevskaya et al., 2013; Ihongo and Wang, 2015; Aslam and Badruddin, 2015; Shirish K. Persai et al., 2019). CRI is therefore predominantly modulated by solar wind dynamics and magnetic field scattering processes (Firoz et al., 2010).

Previous investigations by Munakata et al. (1979), Fujimoto et al. (1983), and Kojima et al. (2007) consistently show that an increase in solar wind velocity leads to a decrease in cosmic ray intensity. The effects of high-speed solar wind streams originating from various sources on galactic cosmic ray modulation have also been studied extensively (Shrivastava and Shukla, 1994; Shrivastava, 1997). The flux of cosmic rays' incident on the Earth's upper atmosphere is modulated by both solar wind conditions and the Earth's magnetic field. Since solar wind properties vary with solar activity across different solar cycles, the level of cosmic ray modulation also changes accordingly (Firoz et al., 2010). Consequently, the degree of cosmic ray modulation is strongly dependent on solar activity. Moreover, heliospheric modulation processes highlight the crucial role of solar wind parameters in triggering various space weather phenomena (Ahluwalia, 2003). Among these processes, enhanced solar wind velocity is one of the dominant factors influencing CRI variation (Sabbah, 2000).

Figures 1.13 and 1.14 present time-series profiles of monthly and annual mean solar plasma speed (VSP) alongside variations in CRI measured by the Oulu and Moscow neutron monitors during solar cycles 23 and 24. The figures clearly indicate contrasting trends between solar wind speed and CRI. During solar cycle 23, the minimum in CRI coincides with the maximum in solar plasma speed. Figures 1.15 and 1.16 further reveal a weak negative correlation during solar cycle 24 (−0.24 for Oulu and −0.14 for Moscow) and a strong negative correlation during solar cycle 23 (−0.56 for Oulu and −0.55 for Moscow). The corresponding linear regression equations are given by:

$$V_{SP} = \alpha+\beta*CRI,$$

where α is the intercept and β is the slope.

Hypothesis testing was performed at the 5% level of significance. Both regression coefficients are statistically significant at the 95% confidence level during solar cycle 23, whereas for solar cycle 24 the slope is not significantly different from zero.

E. Long Term Association of CRI & T_{SP}

For solar cycles 23 and 24, a correlation analysis was carried out between cosmic ray intensity and solar plasma temperature (T_{SP}). Annual mean cosmic ray intensity data from the Oulu and Moscow super neutron monitor stations were used for the analysis. As shown in Figures 1.17 and 1.18, solar plasma temperature and cosmic ray intensity exhibit an anti-correlated behaviour, indicating that increases in T_{SP} correspond to decreases in cosmic ray intensity. Furthermore, the variation pattern of solar plasma temperature closely resembles that of solar plasma speed in relation to cosmic ray intensity.

The study utilizes yearly averaged values of solar plasma temperature and cosmic ray neutron intensity recorded at the Oulu and Moscow neutron monitor stations over the period 1996–2019. Figures 1.19 and 1.20 present the correlation profiles between fluctuations in cosmic ray intensity and the yearly mean solar plasma temperature during solar cycles 23 and 24. The results reveal a strong negative correlation during solar cycle 23, with correlation coefficients of −0.71 for both Oulu and Moscow neutron monitors, respectively. During solar cycle 24, the negative correlation persists but is comparatively weaker, with coefficients of −0.46 for Oulu and −0.38 for Moscow.

The corresponding linear regression equations are given by:

$$T_{SP} = \alpha+\beta*CRI,$$

where α is the intercept and β is the slope.

For solar cycle 23, solar plasma temperature (TSP) explains approximately 50% of the variance in cosmic ray intensity (CRI) observed at both the Oulu and Moscow neutron monitor stations, indicating strong model performance for this cycle. Hypothesis testing was conducted at the 5% significance level, and the regression coefficients were found to be statistically significant at the 95% confidence level. In contrast, for solar cycle 24, the regression slope is not significantly different from zero, rendering the coefficients statistically insignificant. Thus, while TSP shows a significant relationship with CRI during solar cycle 23, this relationship weakens substantially during solar cycle 24.

These results are consistent with the findings of Persai et al. (2019), who reported an anti-correlation between cosmic ray intensity and proton temperature, with correlation strengths dependent on the cutoff rigidity of the neutron monitor station.

F. Long Term Association of CRI & D_{SP}

A correlation study between cosmic ray intensity and solar plasma density (D_{SP}) has been done for solar cycles 23 and 24. The yearly mean results of the Oulu and Moscow super neutron monitors were utilized in a correlative investigation. In figure 1.21 and 1.22, the density of the solar plasma and the intensity of the cosmic rays have lately been in phase with one another. As solar plasma speed, solar plasma temperature, and changes in cosmic ray intensity shift, we have shown that solar plasma density displays the opposite trend. Additionally, we have noted that for solar cycle 23, the lowest values of cosmic rays and solar plasma density are simultaneous. The examination of the relationship between solar plasma density and cosmic ray intensity during solar cycle 24 has revealed more oddities.

Figures 1.23 and 1.24 illustrate the correlation profile between the fluctuation in cosmic ray intensity (measured by the Oulu and Moscow Neutron monitors) and the yearly average value of solar plasma density (D_{SP}) during solar cycles 23 and 24. It is demonstrated that there is a weak and positive relationship with correlation coefficients of 0.38 for both Oulu and Moscow neutron monitors during solar cycle 23 and -0.01 and -0.13 for the Oulu and Moscow neutron monitors during solar cycle 24.

The corresponding linear regression equations are given by:

$$T_{SP} = \alpha+\beta*CRI,$$

where α is the intercept and β is the slope.

At a 5% level of significance, the hypothesis testing was looked at. For solar cycles 23 and 24, we discovered that the slope is not significant from zero. Therefore, it may be argued that none of the coefficients for solar cycles 23 or 24 is statistically significant.

According to study findings by Shirish K. Persai et al. from 2019 that cosmic ray intensity weakly anticorrelated with proton density and correlation coefficient is more for neutron monitor station of high cut off rigidity

IV. DISCUSSION

The results affirm that CRI is predominantly influenced by solar magnetic activity. Stronger correlations in Solar Cycle 24 suggest that the weaker cycle had clearer modulation effects due to lower heliospheric magnetic field turbulence. CME rates, sunspot numbers, and radio flux show the strongest control over CRI, consistent with earlier findings (Cane 2000; Lara et al. 2005; Shrivastava 2007). Solar wind speed and proton temperature, although important for short-term modulation, show inconsistent long-term influence, especially during Cycle 24. Plasma density remains an insignificant factor for long-term CRI modulation.

V. CONCLUSION

This study provides a detailed multi-parameter correlation analysis between cosmic ray intensity and solar–interplanetary features during Solar Cycles 23 and 24. Key conclusions are:

1) CRI shows strong anti-correlation with sunspot numbers, SRF, and CME rates—especially during Solar Cycle 24.
2) Solar wind speed and proton temperature influence CRI moderately in Solar Cycle 23 but insignificantly in Solar Cycle 24.
3) Solar plasma density exhibits weak or no long-term relationship with CRI.
4) Solar activity parameters can explain up to 90% of CRI variability, indicating their dominant role in heliospheric modulation.

These findings help improve understanding of cosmic ray transport and provide valuable input for space weather modeling.

VI. ACKNOWLEDGMENT

We are grateful to the personnel of the world network of Oulu and Moscow neutron monitor station providing data from continuous records of cosmic ray intensity http://cr0.izmiran.ru/oulu & http://cr0.izmiran.ru/mosc/ as well as Omni web data centre (https://omniweb.gsfc.nasa.gov) for the data on sunspot number, solar radio flux, solar wind parameter. We thank the anonymous reviewer's insightful recommendations and remarks, which enabled us to make significant improvements to the manuscript.

REFERENCES

[1] Ahluwalia, H.S., 2003; Geophys. Res. Lett., Vol. 30 (3), 1133
[2] Aslam, O.P.M., Badruddin, 2015; Solar Physics, Vol. 290, p 2333-2353
[3] Bazilevskaya, G.A., Krainev, M.B., Svirzhevskaya, A.K., Sivirzhevsky, N.S., 2013; Cosmic Research, Vol. 51, p 29-36
[4] Cane, H. V., 2000; Space Sci. Rev., Vol. 93, pp. 55-77
[5] Firoj, K.A., Kumar, D.V., Cho, K.S., 2010; Astrophys Space Sci. 325, 185-193
[6] Forbush, S.E., 1958; J. Geophys. Res. 63, 651
[7] Fujimoto, K., Kojima, H., Murakami, K., 1983; 18th ICRC, Vol. 3 (MG Sessions), p 267-269
[8] Ihongo, G.D., Wang, C.H.T., 2015; PoS, ICRC, 508
[9] Kojima, H., et al., 2007; Proc. of the 30th ICRC, Vol. 1, p 561-564
[10] Kota, J., 2013; Space Science Reviews, Vol. 176, p 391- 403
[11] Lange, I., Forbush, S.E., 1957, Carnegie Institution of Washington Publication 175, Washington, DC, U.S.A.
[12] Lara, A., et al., 2005; The Astronomical Journal, Vol. 625, p 441-450.
[13] Mavromichalaki, H., Paouris, E., Karalidi, T., 2007; Solar Physics, Vol. 245, p 369-390.
[14] Mishra, V.K., Tiwari, D.P., Tiwari, C.M., Agrawal, S.P., 2005; Indian Journal of Radio and Space Physics Vol. 34, pp 13-16.
[15] Munakata, Y., Nagashima, K., 1979; 16th ICRC, Vol. 3, p 530-534.
[16] Parker, E.N., 1965; Planetary and Space Science, Vol. 13 (1), p 9-49.
[17] Parker, E.N., 1965; Space Science Reviews, Vol. 4, p 666-708.
[18] Persai, S.K., Jothe, M., Shrivastava, P.K., 2019; Pramana Research Journal, vol. 9 (6), 920 – 928.
[19] Sabbah, I., 2000; Can. J. Phys. 78, 293-302.
[20] Sabbah, I., 2000; Geophysical Research Letters, Vol. 27 (13), p 1823-1826.
[21] Shea, M.A., Smart, D.F., 1985; 19th Intern. Cosmic Ray Conf., Vol. 4, p. 501- 504.
[22] Shrivastava, P.K., 1997; Proc. 25th ICRC, Vol. 1, p 429.
[23] Shrivastava, P.K., 2001; Proc. of the 27th ICRC, Vol. 8, p 3425.

[24] Shrivastava, P.K., Jothe, M.K. & Singh, M., 2011; Solar Physics, 269,401-410.
[25] Shrivastava, P.K., Shukla, R.P., 1993; Proc. 23rd ICRC, Calgary, Vol.3, p.489-492.
[26] Shrivastava, P.K., Shukla, R.P., 1994; Solar Physics, Vol. 154, p 177-185.
[27] Shrivastava, P.K., Shukla, R.P., 1996; Bulletin of the Astronomical Society of India, Vol. 24, p 663.
[28] Shrivastava, P.K.,2007; Asian J. Phys. (India), 1,97.
[29] Simpson, J.A., 1963; Proc. International Conference Cosmic Rays, Jaipur, 155.
[30] Zhao, L.-L., G. Qin, M. Zhang, and B. Heber, 2014; J. Geophys. Res. Space Physics, 119, 1493–1506.

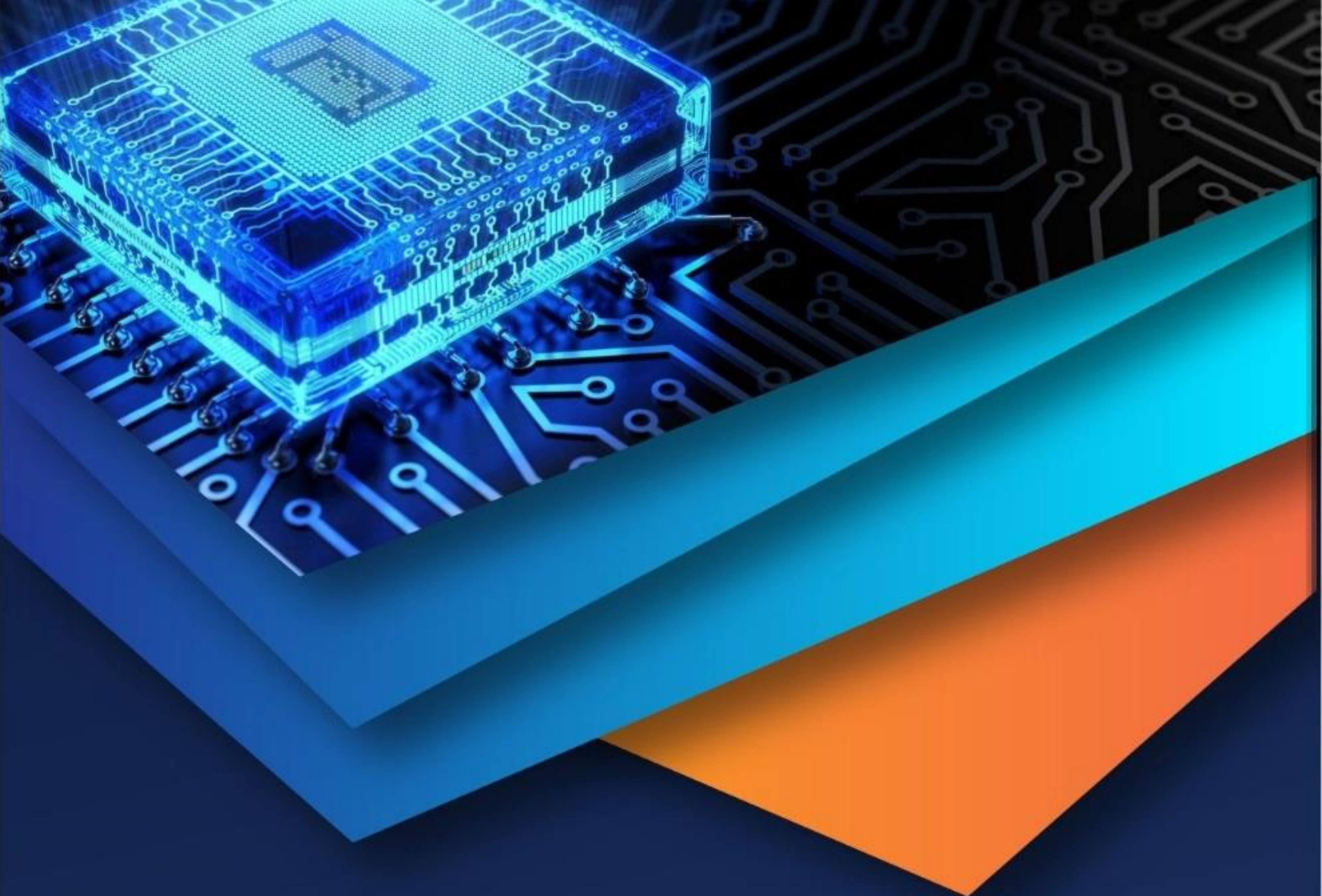

10.22214/IJRASET

INDEX COPERNICUS
45.98

ISRA JIF
IMPACT FACTOR:
7.129

SJIFactor
TOGETHER WE REACH THE GOAL
IMPACT FACTOR:
7.429

ISI

INTERNATIONAL JOURNAL FOR RESEARCH

IN APPLIED SCIENCE & ENGINEERING TECHNOLOGY